

## Self-Assembly of the *Agrobacterium tumefaciens* VirB11 Traffic ATPase

SVETLANA RASHKOVA,<sup>†</sup> XUE-RONG ZHOU,<sup>‡</sup> JUN CHEN, AND PETER J. CHRISTIE\*

Department of Microbiology and Molecular Genetics, The University of Texas—  
Houston Health Sciences Center, Houston, Texas 77030

Received 28 January 2000/Accepted 8 May 2000

**The *Agrobacterium tumefaciens* VirB11 ATPase is a component of a type IV transporter dedicated to T-DNA delivery to plant cells. In this study, we tested a prediction from genetic findings that VirB11 self-associates in vivo. A chimeric protein composed of VirB11 fused to the DNA binding domain of  $\lambda$  cI repressor protein formed dimers, as shown by immunity of *Escherichia coli* to  $\lambda$  superinfection. An allele encoding VirB11 fused at its C terminus to the green fluorescent protein (GFP) exerted strong negative dominance when synthesized in wild-type *A. tumefaciens* cells. Dominance was suppressed by overproduction of native VirB11, suggestive of titrating or competitive interactions between VirB11 and VirB11::GFP. In support of the titration model, a complex of native VirB11 and VirB11::GFP was recovered by precipitation with anti-GFP antibodies from detergent-solubilized *A. tumefaciens* cell extracts. VirB11 was shown by cI repressor fusion and immunoprecipitation assays to interact with VirB11 derivatives encoded by (i) 11 dominant negative alleles, (ii) recessive alleles bearing codon substitutions or deletions in the Walker A nucleotide binding motif, and (iii) alleles corresponding to the 5' and 3' halves of *virB11*. Further immunoprecipitation studies showed a hybrid protein composed of the N-terminal half of VirB11 fused to GFP interacted with mutant proteins exerting dominant effects and with a recessive Walker A deletion mutant ( $\Delta$ GKT174-176). By contrast, a hybrid protein composed of the C-terminal half fused to GFP interacted with mutants exerting dominant effects but not the Walker A mutant protein. Together, these studies establish that VirB11 assembles as homomultimers in vivo via domains residing in each half of the protein. Furthermore, ATP binding appears to be critical for C-terminal interactions required for assembly of productive homomultimers.**

The T-DNA transfer system of *Agrobacterium tumefaciens* is a member of the recently named type IV, or adapted conjugation, secretion systems in gram-negative bacteria (2, 5, 28, 40). These transporters share the property of having evolved from ancestral conjugation systems for novel purposes during the course of infection. Two subfamilies of the type IV transporters can be distinguished on the basis of the exported substrate(s). One subfamily is dedicated to the conjugal transfer of DNA as a nucleoprotein particle. This is a cell contact-dependent event, and transfer can occur across kingdom boundaries, as exemplified by *A. tumefaciens*-mediated delivery of T-DNA to plant cells and of other DNA to yeast, *Neurospora*, and other fungi (4, 8, 11).

The second subfamily exports effector proteins into the extracellular milieu or directly into the cytosols of eukaryotic target cells. Identified in a rapidly expanding number of bacterial pathogens, these transporters are proposed to play diverse roles associated with virulence. The type IV Ptl system of *Bordetella pertussis* directs the six-subunit pertussis toxin, assembled in the periplasm, across the bacterial outer membrane to the extracellular milieu (2). Very recently, *Helicobacter pylori* was reported to use a type IV transporter encoded by the *cag* pathogenicity island to deliver the 145-kDa Cag protein directly to the mammalian host cell (31, 33). CagA undergoes tyrosine phosphorylation, forms a cylindrical structure, and

appears to induce cytoskeletal rearrangements upon transfer to the host cell (31). Facultative intracellular pathogens including *Legionella pneumophila*, *Rickettsia prowazekii*, *Brucella* spp., and *Bartonella* spp. are thought to export factors that promote survival within macrophages, contribute to phagolysosome fusion, and/or contribute to macrophage killing (23, 32, 35).

Significant progress has been made toward definition of the structure and function of the *A. tumefaciens* T-DNA transfer system (4, 8, 40). Composed of the VirB proteins, the T-DNA transporter likely assembles as a transenvelope channel through which T-DNA is translocated and a pilus for establishing productive interactions with target cells. A subset of VirB protein interactions, key early steps in transporter biogenesis, major and minor pilin subunits, and the pilus structure have been identified (4, 8, 13, 21, 29).

Our laboratory has been investigating the roles of the cytoplasmic membrane ATPases VirB4 and VirB11 in T-DNA transfer (1, 4, 6, 7, 26, 38). VirB11 is related throughout its length to proposed subunits of other type IV transporters and to a number of archaeal proteins of unknown function. In addition, a region of VirB11 that spans the conserved Walker A and B nucleotide binding motifs and an adjacent His box is closely related to corresponding regions of the type II secretion pathway GspE family of proteins (27). Mutations of the conserved Walker A motifs of the VirB11 and GspE family members invariably abolish activities of the cognate systems, and ATP binding and hydrolysis has been confirmed for purified VirB11 (6) and VirB11-like proteins associated with conjugation including TrwD (20a, 27), TrbB, and *H. pylori* HP0525 (20a). Therefore, these proteins most probably share the general property of supplying energy from ATP hydrolysis to drive organellar assembly or substrate translocation at the gram-negative cell envelope.

Mutations of the VirB11 Walker A motif are recessive (26). However, a screen of *virB11* alleles generated by PCR mu-

\* Corresponding author. Mailing address: Department of Microbiology and Molecular Genetics, The University of Texas—Houston Health Sciences Center, 6431 Fannin, Houston, TX 77030. Phone: (713) 500-5440. Fax: (713) 500-5499. E-mail: christie@utmmg.med.uth.tmc.edu.

<sup>†</sup> Present address: Department of Biology, Massachusetts Institute of Technology, Cambridge, MA 02139.

<sup>‡</sup> Present address: CSIRO Plant Industry, Canberra, ACT 2601, Australia.

togenesis resulted in the isolation of 11 dominant alleles (38). Of considerable interest, these alleles fell into two classes, one that coded for nonfunctional VirB11 proteins and a second that coded for fully functional proteins when synthesized in the absence of native VirB11. Isolation of this latter mutant class, which exhibit a phenotype only when synthesized in the presence of native VirB11, prompted a model that a functional T-complex transport system is composed of more than one VirB11 subunit (38). In the present report, we supply further biochemical and molecular genetic evidence for VirB11 self-association *in vivo*.

## MATERIALS AND METHODS

**Enzymes, chemicals, and reagents.** Restriction endonucleases were purchased from Promega (Madison, Wis.), New England Biolabs (Beverly, Mass.), or Gibco-BRL (Grand Island, N.Y.). Klenow fragment of *Escherichia coli* DNA polymerase I and T4 DNA ligase were from Promega. Isopropyl- $\beta$ -D-thiogalactopyranoside, (IPTG), phenylmethylsulfonyl fluoride, carbenicillin, kanamycin, Triton X-100 (TX-100), Coomassie brilliant blue R250, *p*-nitroblue tetrazolium, and 5-bromo-4-chloro-3-indolylphosphate were purchased from Sigma Chemical Co. (St. Louis, Mo.). Acetosyringone (3',5'-dimethoxy-4'-hydroxyacetophenone; AS) was from Aldrich (Milwaukee, Wis.). Alkaline phosphatase-conjugated goat anti-rabbit immunoglobulin G (IgG) and a Bradford protein assay kit were from Bio-Rad Laboratories (Hercules, Calif.). Protein A-Sepharose CL-4B beads were from Pharmacia Biotech (Piscataway, N.J.).

**Bacterial strains, plasmids, phages, and growth conditions.** The bacterial strains, plasmids, and phages used in this study and their relevant characteristics are listed in Table 1. Except where noted, ColE1 plasmids ligated to an IncP plasmid for introduction into *A. tumefaciens* were given the ColE1 plasmid name plus a "B" to designate broad-host-range. *E. coli* strains were maintained on Luria-Bertani (LB) medium. *A. tumefaciens* strains were maintained on MG/L or on AB minimal salts medium (15). Media were supplemented with antibiotics (concentration in micrograms per milliliter) as follows: chloramphenicol for *E. coli* (35), carbenicillin (50), kanamycin (50), tetracycline (5), carbenicillin (100), and kanamycin (100).

For induction of *vir* genes, *A. tumefaciens* cells were grown in MG/L medium to an optical density at 600 nm (OD<sub>600</sub>) of 0.5, harvested by centrifugation, and inoculated at an initial OD<sub>600</sub> of 0.2 into induction medium (AB minimal salts medium [pH 5.5], containing 1 mM phosphate and supplemented with 200  $\mu$ M AS) (15). Cultures were incubated with shaking for 18 h at 20°C and harvested for protein analysis.

**Recombinant DNA techniques.** All procedures for plasmid DNA isolation and manipulation were performed as previously described (14, 15). PCR amplification was performed with a Perkin-Elmer Cetus DNA thermocycler with *Taq* DNA polymerase from Perkin-Elmer (Madison, Wis.). Oligonucleotides were synthesized with a BioSearch 8600 DNA synthesizer. Plasmids were introduced into *A. tumefaciens* strains by electroporation with a Bio-Rad electroporator. For plasmid pXZ41, the  $\sim$ 48 reverse primer and an oligonucleotide (CCGTCAG AGCATGTCAATCAGTG) were used along with pSR5 as a template for PCR amplification of a 450-bp fragment of *virB11* coding for amino acids 157 to 302. For pXZ42, an oligonucleotide (TTGCTGGGCCATATGCGCGAC) and the T3 primer were used along with pSR1 as a template for PCR amplification of a 755-bp fragment coding for amino acids 245 to 343. The cycling parameters were 30 cycles of 94°C for 30 s, 55°C for 30 s, and 72°C for 45 s. Amplified *virB11* [157-302] and *virB11* [245-343] were cloned as an *NdeI*-*XbaI* and *NdeI*-*XhoI* fragments, respectively, in pBSK<sup>+</sup>-*NdeI*. To introduce *virB11.343::gfp* at the *virB11* locus of the Ti plasmid by Campbell-type recombination, A348 cells were transformed by electroporation with pXZ2, which cannot replicate autonomously in *A. tumefaciens*. Carbenicillin-resistant transformants with pXZ2 integrated into the Ti plasmid coexpressed *virB11.343::gfp* from the native *virB* promoter and *virB11* from a separate *virB* promoter as a result of the recombination event.

**Protein analysis and immunoblotting.** Protein concentrations were determined with a Bradford protein assay kit, using bovine serum albumin (Sigma) as the standard. Protein samples were resolved by sodium dodecyl sulfate polyacrylamide gel electrophoresis (SDS-PAGE) and transferred to nitrocellulose membranes, and proteins were visualized by development of blots with anti-VirB11 antiserum and goat anti-rabbit antibodies conjugated to alkaline phosphatase. Purified His<sub>6</sub>-VirB11 was used for raising anti-VirB11 antiserum in New Zealand White rabbits by Cocalico Biologicals, Inc. (Reamstown, Pa.). Anti-VirB11 antibodies were purified by passing the antiserum through an immunoaffinity column of His<sub>6</sub>-VirB11 immobilized on cyanogen bromide-activated Sepharose 4B beads (Pharmacia Biotech). Anti-green fluorescent protein (GFP) antiserum was kindly provided by W. Margolin.

**Virulence assays.** *A. tumefaciens* strains were tested for virulence on uniformly wounded *Kalanchoe daigremontiana* leaves. Controls for the tumorigenesis assays included coinoculation of the same leaf with wild-type A348 and the *virB11* gene deletion strain, PC1011. Virulence was scored in terms of tumor size and time course of tumor appearance. Assays were repeated at least four times for each

strain on separate leaves. Tumors were photographed 4 to 5 weeks after inoculation.

**Phage immunity assay.** *E. coli* AG1688 strains expressing wild-type or chimeric repressors were cross-streaked against  $\sim 10^7$  PFU of the lytic phage  $\lambda$ KH54 spread on half of the surface of LB agar plates. After overnight incubation at 37°C, cross-streaks were examined visually for bacterial growth in the presence of the phage. Immunity was determined as the ability of strains to grow in the presence of phage. As a control for efficient phage infection, strains were cross-streaked against phage  $\lambda$ imm<sup>21c</sup> (17, 18).

**Overexpression of His<sub>6</sub>-VirB11.** One hundred microliters of an overnight culture of *E. coli* BL21( $\lambda$ DE3, pPC9119) was inoculated into 50 ml of LB medium with 50  $\mu$ g of carbenicillin/ml. The culture was grown with shaking at 37°C for 2 h to an OD<sub>600</sub> of  $\sim$ 0.4. Expression of *his<sub>6</sub>-virB11* from the T7 *lac* promoter was induced with 1 mM IPTG for 3 h. Rifampin (200  $\mu$ g/ml) was added to inhibit transcription from the host RNA polymerase. Cells were then collected by centrifugation at 10,000  $\times g$  for 10 min at 4°C. Cell pellets were washed twice with ice-cold 25 mM HEPES pH 8.0 (HEPES buffer), and the cell pellets were stored at  $-70^\circ\text{C}$ .

**Purification of His<sub>6</sub>-VirB11 by IMAC.** Cell pellets were thawed on ice and resuspended in 2.4 ml of HEPES buffer supplemented with 12.5% sucrose, DNase (0.2 mg/ml), and RNase (0.2 mg/ml). An equal volume of 2 $\times$  radioimmunoprecipitation assay buffer (50 mM HEPES [pH 8.0], 300 mM NaCl, 0.2% SDS, 2% NP-40, 2% sodium deoxycholate) was added, and the cell suspension was incubated for 1 h at 4°C. The cell lysates were centrifuged at 14,000  $\times g$  for 45 min. Pelleted material was resuspended in 3 ml of 5 M urea-5 mM imidazole-0.5 M NaCl-25 mM HEPES (pH 8.0) and incubated at room temperature for 1 h with shaking. Unsolubilized material was removed by centrifugation at 14,000  $\times g$  for 15 min. VirB11 was purified by immobilized metal ion affinity chromatography (IMAC) as instructed by the manufacturer (Novagen, Madison, Wis.). Purified protein was obtained at a yield of 0.10 to 0.15 mg of induced culture/ml.

**Immunoprecipitation under nondenaturing conditions.** AS-induced cultures (500 ml) at an OD<sub>600</sub> of 0.7 to 0.8 were pelleted, and cell pellets were washed twice in ice-cold HEPES buffer. Cells were resuspended in 3.5 ml of HEPES buffer supplemented with 20% sucrose, 0.2 mM dithiothreitol, DNase (0.2 mg/ml), and RNase (0.2 mg/ml). Lysozyme was added to a final concentration of 0.4 mg/ml, and cells were incubated for 15 min on ice. Cells were disrupted by three passages through a French press at 14,000 lb/in<sup>2</sup>, and the volume of the cell lysate was brought up to 5 ml with HEPES buffer. The lysate was centrifuged twice at 14,000  $\times g$  for 30 and 15 min, respectively, to remove unbroken cells and cell debris. The concentration of the total cellular protein was adjusted to 1 mg of protein/ml by addition of HEPES buffer. Membranes were solubilized by addition of an equal volume of 2% TX-100-25 mM HEPES (pH 8.0) or 2% TX-100-300 mM NaCl-25 mM HEPES (pH 8.0), followed by incubation at 4°C for 4 h with constant inversion. The solubilized lysates were spun at 100,000  $\times g$  for 1 h in a model TL-100 ultracentrifuge (Beckman Instruments, Fullerton, Calif.). Anti-GFP antiserum was added to 1 ml of the cleared supernatant at a titer of 1:1,000, and the mixture was incubated for 2 h at 4°C with shaking. Protein A-Sepharose beads (3 mg/sample) presoaked in solubilization buffer were added, and incubation was continued for 2 h at 4°C with shaking. Beads were pelleted by centrifugation at 20,000  $\times g$  for 30 s, washed three times in solubilization buffer, resuspended in 50  $\mu$ l of 2 $\times$  protein sample buffer (3% SDS, 5%  $\beta$ -mercaptoethanol, 0.1% bromophenol blue, 20% glycerol, 50 mM HEPES [pH 6.8]), and boiled for 5 min. Beads were pelleted by centrifugation at 20,000  $\times g$  for 30 s, and supernatants were analyzed by SDS-PAGE and immunoblotting.

## RESULTS

**Dominance of *virB11.343::gfp* and suppression by VirB11 overproduction.** To assay for VirB11 self-association *in vivo*, we fused full-length VirB11 to GFP for use in immunoprecipitation studies. In preliminary studies, we determined that *virB11.343::gfp* exerts negative dominance, resulting in severely attenuated virulence of cells coexpressing *virB11.343::gfp* and wild-type *virB11* (Fig. 1). *virB11.343::gfp* expression failed to restore virulence of the  $\Delta$ *virB11* mutant, PC1011. This allele therefore is a member of the class II dominant *virB11* alleles that code for nonfunctional VirB11 mutants (38). A348(pXZB63) expressing *gfp* exhibited wild-type virulence, showing that GFP does not interfere with T-DNA transport. *A. tumefaciens* cells carrying pXZB2 synthesized a protein of  $\sim$ 58 kDa, the expected size of the VirB11.343::GFP fusion protein, that coreacted with anti-VirB11 and anti-GFP antiserum (Fig. 2A, lanes 1, 3, 5, 6, and 11). The anti-VirB11 and anti-GFP antisera did not cross-react with native GFP (lanes 7 and 8) and VirB11 (lanes 9 and 10), respectively.

Merodiploid cells accumulated appreciably more VirB11.343::GFP than VirB11 (Fig. 2A), attributable to differences in copy

TABLE 1. Bacterial strains, phages, and plasmids used

Strain, phage, or plasmid	Relevant characteristics	Source or reference
<i>E. coli</i>		
DH5 $\alpha$	$\lambda^-$ $\phi$ 80d/ <i>lacZ</i> $\Delta$ M15 $\Delta$ ( <i>lacZYA-argF</i> ) <i>U169 recA1 endA1 hsdR17</i> ( $r_K^- m_K^+$ ) <i>supE44 thi-1 gyrA relA1</i>	GIBCO-BRL
BL21( $\Delta$ DE3)	F $^-$ <i>ompT</i> ( $r_B^- m_B^-$ )	Novagen
AG1688	MC1061 F $^+$ 128 <i>lacI<sup>a</sup> lacZ::Tn5</i>	J. Hu
<i>A. tumefaciens</i>		
A136	Strain C58 cured of pTi plasmid	37
A348	A136 containing pTiA6NC	16
PC1011	A348 derivative deleted of <i>virB11</i> from pTiA6NC	1
PC1000	A348 deleted of <i>virB</i> operon from pTiA6NC	14
PC2111	A348 derivative with pXZ2 integrated into pTiA6NC; expresses <i>virB11.343::gfp</i> and <i>virB11</i> from Ti plasmid	This study
Bacteriophages		
$\lambda$ KH54	Lambda phage deleted of <i>cI</i>	J. Hu
$\lambda$ imm $^{21c}$	<i>cI</i> $^-$ lambda; immunity region substitution	J. Hu
Plasmids		
Vectors		
pSW172	Tet $^r$ , IncP plasmid containing P $_{lac}$ with downstream polylinker sequence	3
pSW213	Tet $^r$ , IncP plasmid containing <i>lacI<sup>a</sup></i> and P $_{lac}$ with polylinker sequence	3
pXZ151	Kan $^r$ , pSW172 with Kan $^r$ gene	39
pTJS75-kan	Kan $^r$ , IncP vector	19
pBSIISK $^+$ <i>NdeI</i>	Crb $^r$ , cloning vector	1
pBSIISK $^+$ <i>NcoI</i>	Crb $^r$ , cloning vector	39
pUC4K	Source of Kan $^r$ cassette	Pharmacia
<i>virB11</i> expression plasmids		
pPC9119	Crb $^r$ , pET15b (Novagen) expressing <i>his<math>_6</math>-virB11</i> from P $_{T7 lac}$	26
pPC7113	Crb $^r$ , pUC118 with <i>virB11K175Q</i> expressed from P $_{lac}$	26
pED11	Tet $^r$ , pTJS75-tet carrying <i>virB11</i> downstream of P $_{virB}$	36
pXZ1	Crb $^r$ , 1.00-kb <i>NdeI-XhoI</i> fragment from a PCR product carrying <i>virB11</i> without a TAG stop codon, inserted into similarly digested pPC914KS $^+$	This study
pXZ2	Crb $^r$ , 0.70-kb <i>XhoI-KpnI</i> fragment carrying <i>gfp</i> from pXZ5 inserted into similarly digested pXZ1, making <i>virB11.343::gfp</i>	This study
pXZ5	Crb $^r$ , pUC118 with ~0.75-kb <i>HindIII-BamHI</i> fragment carrying <i>gfp</i> gene	This study
pXZ41	Crb $^r$ , 0.48-kb <i>NdeI-XbaI</i> fragment carrying <i>virB11[157-302]</i> generated by PCR amplification (see Materials and Methods) inserted into pBSK $^+$ <i>NdeI</i> downstream of P $_{lac}$	This study
pXZ42	Crb $^r$ , 0.65-kb <i>NdeI-XhoI</i> fragment carrying <i>virB11[245-343]</i> generated by PCR amplification inserted into pBSK $^+$ <i>NdeI</i> downstream of P $_{lac}$	This study
pXZ63	Crb $^r$ , 0.72-kb <i>SacI-KpnI</i> fragment carrying <i>gfp</i> from pCSK100 (22) inserted into similarly digested pBSK $^+$ <i>NdeI</i>	This study
pSR1	Crb $^r$ , pBSK $^+$ <i>NdeI</i> with <i>virB11</i> expressed from P $_{virB}$	26
pXZB95	Crb $^r$ , Kan $^r$ ; pSR1 digested with <i>XhoI</i> and ligated to pTJS75-kan digested with <i>SalI</i> ; <i>virB11</i> is downstream of P $_{virB}$	This study
pSR2	Crb $^r$ , pBSIISK $^+$ <i>NcoI</i> with <i>his<math>_6</math>-virB11</i> expressed from P $_{lac}$	26
pSR4	Crb $^r$ , pSR1 derivative with <i>virB11[1-157]</i> expressed from P $_{virB}$	26
pSR5	Kan $^r$ Cam $^r$ , pBKS $^+$ with <i>virB11[157-343]</i> expressed from P $_{lac}$	26
pSR33	Kan $^r$ , 2.30-kb <i>XbaI-KpnI</i> fragment carrying P $_{virB}$ <i>virB11.343::gfp</i> from pXZ2 inserted into similarly digested pXZ151	This study
pSR40	Crb $^r$ , 1.42-kb <i>BamHI-KpnI</i> fragment from pPC7113 inserted into similarly digested pPC9114, substituting <i>virB11K175Q</i> for <i>virB11</i> downstream of P $_{virB}$	This study
pSR41	Crb $^r$ , 1.42-kb <i>BamHI-KpnI</i> fragment from pPC7112 inserted into similarly digested pPC9114, substituting <i>virB11<math>\Delta</math>174-176</i> for <i>virB11</i> downstream of P $_{virB}$	This study
pSR43	Crb $^r$ , 0.73-kb <i>XhoI-KpnI</i> fragment carrying <i>gfp</i> from pXZ2 inserted into similarly digested pSR4, making <i>virB11[1-157]::gfp</i>	This study
pSR44	Crb $^r$ , 0.85-kb <i>BglII-KpnI</i> fragment carrying <i>gfp</i> from pXZ2 inserted into similarly digested pSR5, making <i>virB11[157-343]::gfp</i>	This study
pSR47	Kan $^r$ , 2.30-kb <i>XbaI-KpnI</i> fragment carrying P $_{virB}$ <i>virB11K175Q</i> from pSR40 inserted into similarly digested pXZ151	This study
pSR48	Kan $^r$ , 2.30-kb <i>XbaI-KpnI</i> fragment carrying P $_{virB}$ <i>virB11<math>\Delta</math>GKT174-176</i> from pSR41 inserted into similarly digested pXZ151	This study
pSR49	Crb $^r$ , 0.85-kb <i>BglII-KpnI</i> fragment carrying <i>gfp</i> from pXZ2 inserted into similarly digested pSR5, making <i>virB11K175Q::gfp</i>	This study
pSR50	Crb $^r$ , 0.85-kb <i>BglII-KpnI</i> fragment carrying <i>gfp</i> from pXZ2 inserted into similarly digested pSR5, making <i>virB11<math>\Delta</math>GKT174-176::gfp</i>	This study
pSR51	Crb $^r$ , pBSK $^+$ <i>NcoI</i> with <i>his<math>_6</math>-virB11<math>\Delta</math>GKT174-176</i> expressed from P $_{lac}$	This study
pSR70	Crb $^r$ Tet $^r$ , pED11-pXZ2 cointegrate expressing <i>virB11</i> and <i>virB11.343::gfp</i>	This study
pSR71	Crb $^r$ Tet $^r$ , pED11-pXZ63 cointegrate expressing <i>virB11</i> and <i>gfp</i>	This study
pSR74	Kan $^r$ Crb $^r$ , pSR47-pXZ2 cointegrate expressing <i>virB11K175Q</i> and <i>virB11.343::gfp</i>	This study
pSR75	Kan $^r$ Crb $^r$ , pSR48-pXZ2 cointegrate expressing <i>virB11<math>\Delta</math>GKT174-176</i> and <i>virB11.343::gfp</i>	This study
pSR76	Kan $^r$ Crb $^r$ , pSR47-pSR49 cointegrate expressing <i>virB11.K175Q</i> and <i>virB11K175Q::gfp</i>	This study
pSR77	Kan $^r$ Crb $^r$ , pSR48-pSR50 cointegrate expressing: <i>virB11<math>\Delta</math>GKT174-176</i> and <i>virB11<math>\Delta</math>GKT174-176::gfp</i>	This study
pSR78	Crb $^r$ Tet $^r$ , pED11-pSR43 cointegrate expressing <i>virB11</i> and <i>virB11[1-157]::gfp</i>	This study
pSR79	Crb $^r$ Tet $^r$ , pED11-pSR44 cointegrate expressing <i>virB11</i> and <i>virB11[157-343]::gfp</i>	This study

Continued on following page

TABLE 1—Continued.

Strain, phage, or plasmid	Relevant characteristics	Source or reference
pXZ1101–pXZ1110 pSR81–pSR90	Crb <sup>f</sup> , pBSK <sup>+</sup> <i>NdeI</i> expressing dominant <i>virB11</i> alleles from P <sub>virB</sub> . Kan <sup>r</sup> Crb <sup>f</sup> , pSR33 expressing <i>virB11.343::gfp</i> ligated at its <i>KpnI</i> site to each of the pXZ1101 plasmids expressing the dominant <i>virB11</i> alleles. Plasmid numbers correspond to dominant alleles 1–10 (38)	38 This study
<i>cI</i> expression plasmids		
pJH391	Crb <sup>f</sup> , a pBR322-based clone containing <i>cI ind1</i> residues 1–132 expressed from P <sub>lacUV5</sub> for construction of <i>cI'</i> hybrid proteins	17
pJH157	Crb <sup>f</sup> , pJH391 carrying the intact <i>cI ind1</i> downstream of P <sub>lacUV5</sub>	17
pKH101	Crb <sup>f</sup> , pJH391 carrying <i>cI[1-102]</i> downstream of P <sub>lacUV5</sub>	17
pZ150	Crb <sup>f</sup> , pBR322 with an M13 single-strand origin	J. Hu
pSR58	Crb <sup>f</sup> , pJH391 with <i>NdeI</i> at bp 4482 eliminated by <i>NdeI</i> digestion and blunt ending with Klenow fragment of <i>E. coli</i> DNA polymerase	7
pTAD180	Crb <sup>f</sup> , 1.20-kb <i>HindIII-SalI</i> fragment carrying <i>virB11</i> from pPC9114 inserted into similarly digested pSR58, making <i>cI'</i> fused at codon 117 to the 5' end of <i>virB11</i>	7
pSR61	Crb <sup>f</sup> , 0.58-kb <i>NdeI-XhoI</i> fragment carrying <i>virB11[1-157]</i> from pSR4 inserted into similarly digested pTAD180, making <i>cI'::virB11[1-157]</i>	This study
pSR62	Crb <sup>f</sup> , 0.96-kb <i>NdeI-XhoI</i> fragment carrying <i>virB11[157-343]</i> from pSR5 inserted into similarly digested pTAD180, making <i>cI'::virB11[157-343]</i>	This study
pSR63	Crb <sup>f</sup> , 0.45-kb <i>NdeI-XhoI</i> fragment carrying <i>virB11[157-302]</i> from pXZ41 inserted into similarly digested pTAD180, making <i>cI'::virB11[157-302]</i>	This study
pSR64	Crb <sup>f</sup> , 0.70-kb <i>NdeI-XhoI</i> fragment carrying <i>virB11[245-343]</i> from pXZ42 inserted into similarly digested pTAD180, making <i>cI'::virB11[245-343]</i>	This study
pSR66	Crb <sup>f</sup> , 1.42-kb <i>NdeI-XhoI</i> fragment carrying <i>virB11</i> from pPC9118 (1) inserted into similarly digested pTAD180, making <i>cI'::virB11</i>	This study
pSR68	Crb <sup>f</sup> , ~1-kb <i>NdeI-XhoI</i> fragment carrying <i>virB11K175Q</i> from pSR40 inserted into pTAD180, making <i>cI'::virB11K175Q</i>	This study
pSR69	Crb <sup>f</sup> , ~1-kb <i>NdeI-XhoI</i> fragment carrying <i>virB11ΔGKT174-176</i> from pSR42 inserted into pTAD180, making <i>cI'::virB11ΔGKT174-176</i>	This study
pSR91–pSR100	Crb <sup>f</sup> , ~1-kb <i>NdeI-XhoI</i> fragments carrying the dominant <i>virB11</i> alleles from the pXZLx plasmid series inserted into pTAD180, making <i>cI'</i> fusions to the dominant <i>virB11</i> alleles. Plasmid numbers correspond to dominant alleles 1–10 (38)	This study

numbers of the IncP (5 to 10 copies per cell) and Ti plasmids (1 to 2 copies per cell). To test whether dominance could be suppressed by enhanced production of VirB11, PC2111 merodiploid cells were engineered to express *virB11.343::gfp* and *virB11* from the Ti plasmid with or without additional *virB11* expression from an IncP replicon. For an unknown reason, PC2111 merodiploid cells with or without the pTJS75-tet vector plasmid accumulated lower levels of VirB11 than VirB11::GFP and exhibited attenuated virulence (data not shown). However, PC2111(pED11) expressing *virB11* from the Ti plasmid and an IncP replicon accumulated VirB11 at >2-fold-higher levels than VirB11.343::GFP, as determined by densitometry scanning of the immunoblot (Fig. 2A, lane 13). The inability to significantly overproduce VirB11 could be due to a previously observed stabilization of VirB11 by other Ti plasmid-encoded VirB proteins (1). Even so, PC2111(pED11) induced formation of nearly wild-type tumors (Fig. 1). The finding that VirB11 overproduction suppressed dominance suggests the VirB11.343::GFP hybrid exerts its negative effect by sequestering available VirB11 into nonproductive complexes. Alternatively, the hybrid protein might compete with native VirB11 for another component of the transport machine.

**VirB11.343::GFP and VirB11 form a mixed multimer.** To test for interactions between VirB11.343::GFP and VirB11, anti-GFP antiserum was used to immunoprecipitate GFP-containing complexes from lysates of A348 and PC1000 strains synthesizing VirB11, VirB11.343::GFP, and/or GFP. As shown in Fig. 2B, native VirB11 coprecipitated with VirB11.343::GFP when these proteins were synthesized both in the presence and in the absence of other transfer system components (lanes 1 and 3). By contrast, VirB11 was not detected in precipitates

when synthesized in the absence of the fusion protein (lanes 2 and 4) or when cosynthesized with GFP (lanes 7 and 8). Pre-immune GFP antiserum did not precipitate either the fusion protein or native VirB11 (lanes 9 and 10). Together, these findings demonstrate that VirB11 and VirB11.343::GFP form mixed multimers independent of the presence of other VirB proteins. We attempted to further confirm VirB11 multimerization by coexpressing alleles for native VirB11 and a functional, N-terminally His-tagged form of VirB11 in *A. tumefaciens*. Upon detergent solubilization of membranes and IMAC, we reproducibly detected abundant levels of both the 38-kDa VirB11 and 40-kDa His-VirB11 species in the column eluates. However, a low level of native VirB11 also was retained on Ni<sup>2+</sup> or Co<sup>2+</sup> affinity columns upon chromatography of extracts from cells expressing wild-type *virB11* in the absence of

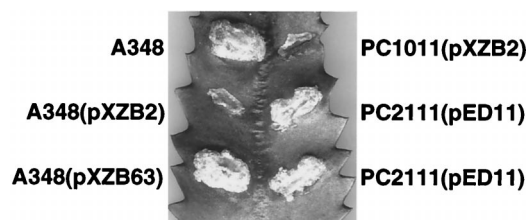


FIG. 1. *virB11.343::gfp* dominance and suppression by VirB11 overproduction. *A. tumefaciens* strains expressing wild-type *virB11*, *gfp*, and/or *virB11.343::gfp* were assayed for virulence by inoculation onto wounded *K. daigremontiana* leaves. A348, wild type; PC1011,  $\Delta virB11$  mutant; PC2111, A348 merodiploid expressing *virB11* and *virB11.343::gfp* from the Ti plasmid. Broad-host-range plasmids and relevant genes expressed: pXZB2 (P<sub>lac::virB11.343::gfp</sub>), pXZB63 (P<sub>lac::gfp</sub>), pED11 (P<sub>virB11::virB11</sub>).

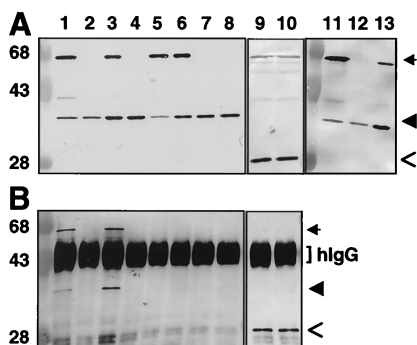


FIG. 2. Coprecipitation of VirB11 and VirB11.343::GFP. (A) TX-100-solubilized proteins were subjected to SDS-PAGE and immunostaining with anti-VirB11 (lanes 1 to 8 and 11 to 13) or anti-GFP (lanes 9 and 10) antiserum. (B) Immunoprecipitates of protein extracts shown in panel A, immunoprecipitated with anti-GFP antiserum (lanes 1 to 4 and 7 to 10) or with preimmune serum (lanes 5 and 6). Lanes: 2, 4, and 12, wild-type A348 expressing *virB11* (from pTi); 1, 5, and 11, A348(pXZB2) expressing *virB11* (pTi) and *virB11.343::gfp* (IncP); 7 and 9, A348(pXZB63) expressing *virB11* (pTi) and *gfp* (IncP); 3 and 6, the *virB* operon deletion strain, PC1000(pSR70), expressing *virB11.343::gfp* (IncP) and *virB11* (IncP); 8 and 10, PC1000(pSR71) expressing *virB11* (IncP) and *gfp* (IncP); 13, PC2111(pED11) expressing *virB11* (pTi and IncP) and *virB11.343::gfp* (pTi). hIgG, immunoreactive heavy chain of IgG. Arrows indicate positions of VirB11::GFP, arrowheads denote VirB11, and open arrows denote GFP. Positions of molecular weight markers are shown at the left, with sizes in kilodaltons indicated.

*his-virB11*. This residual binding of native VirB11 to the columns prevented use of IMAC to confirm VirB11 multimerization (data not shown).

**VirB11 confers dimerization of the  $\lambda$ cI repressor DNA-binding domain.** To gain independent evidence for VirB11 self-association, we used the  $\lambda$ cI repressor fusion system. cI repressor protein functions as a homodimer, each monomer consisting of an N-terminal DNA binding and a C-terminal dimerization domain. The N-terminal domain (cI') by itself binds operator sites poorly and is ineffective in preventing expression of early lytic pathway genes. The C-terminal domain, or substitutions of this domain with heterologous dimerizing proteins or domains, strongly promotes cI dimerization and operator site binding and thus confers immunity to  $\lambda$  superinfection (17, 18).

To test whether VirB11 could serve as a dimerization domain for the cI repressor, we constructed a gene fusion, cI':*virB11*, composed of sequence coding for the N-terminal cI domain fused to the complete *virB11* coding sequence. Equivalent plasmid constructs carrying cI':*virB11* (pSR66; cI':VirB11), full-length cI (pJH157; *ind1*), sequence for the N-terminal 102 residues of cI (pKH101; cI 1-102), or vector only (pZ150) were introduced into *E. coli* AG1688 cells, and the regulatory properties of the repressor constructs were compared by cross-streak analysis against phage  $\lambda$ KH54. Bacterial cells carrying pSR66 or pJH157 were immune to infection by  $\lambda$ KH54, whereas those carrying pKH101 or pZ150 were sensitive (Fig. 3A). To test for the presence of the  $\lambda$  phage receptor, strains were cross-streaked against phage  $\lambda$ imm<sup>21c</sup>, a phage derivative with a substitution of the immunity region such that the cI repressor cannot repress its lytic development (Fig. 3B). The sensitivity of strains to  $\lambda$ imm<sup>21c</sup> confirmed the expression of the  $\lambda$  phage receptor in the cells. We attempted to inhibit cI dimer formation by synthesis of native VirB11 from a compatible IncP replicon but were unable to reproducibly detect conversion of host cells to  $\lambda$ KH54 sensitivity. One explanation is that the abundance of the native protein was insufficient for titrating the cI':VirB11 fusion proteins. Another possibility

consistent with chemical cross-linking data (25) and results of a recent study of the VirB11 homolog TrbB (20) is that VirB11 assembles as higher-order homo-oligomers in vivo. If so, higher-order mixed multimers of VirB11 and cI':VirB11 might retain the capacity to bind efficiently to cI operator sites.

**Self-interaction of VirB11 mutants.** VirB11 requires an intact Walker A motif for function in DNA export. Alleles with Walker A codon substitutions or deletions are recessive, which could be due to a failure of these mutant proteins to oligomerize. To examine whether nucleoside triphosphate binding or hydrolysis is required for VirB11 self-assembly, the K175Q and  $\Delta$ GKT174-176 alleles were coexpressed with *virB11.343::gfp* in PC1000 cells, and the resulting cell lysates were subjected to immunoprecipitation with anti-GFP antiserum. We also fused the K175Q and  $\Delta$ GKT174-176 alleles at their 3' ends to *gfp* and coexpressed these chimeric genes with the K175Q and  $\Delta$ GKT174-176 alleles, respectively. As summarized in Table 2, the Walker A mutant proteins coprecipitated with VirB11.343::GFP. In addition, the K175Q and  $\Delta$ GKT174-176 mutant proteins coprecipitated with the K175Q::GFP and  $\Delta$ GKT174-176::GFP fusion proteins, respectively. The Walker A mutant proteins were not detected in material precipitated from strains lacking the GFP fusion proteins (Table 2) (25).

We further tested for the ability of K175Q and  $\Delta$ GKT174-176 to self-associate with the cI repressor fusion system. *E. coli* AG1688 strains with pSR68 expressing cI':*virB11K175Q* and pSR69 expressing cI':*virB11 $\Delta$ GKT174-176* each grew in the presence of phage  $\lambda$ KH54, suggesting that the Walker A mutants mediate cI repressor dimerization (Table 2) (25). Together, these findings show that VirB11 minimally can dimerize independently of ATP binding or hydrolysis.

Next, we assayed for interactions between VirB11 and mutant proteins exerting negative dominance previously shown to be suppressible by VirB11 overproduction (38). One class of dominant alleles (class II) encodes nonfunctional VirB11 mutants, whereas a second class (class III) encoded VirB11 derivatives that exhibited wild-type function when expressed in the absence of the native protein. Thus, if oligomerization is a prerequisite for VirB11 function, at least the latter class of mutants was expected to self-assemble. To test this prediction, extracts from PC1000 cells engineered to coexpress *virB11.343::gfp* and one of the dominant alleles were subjected

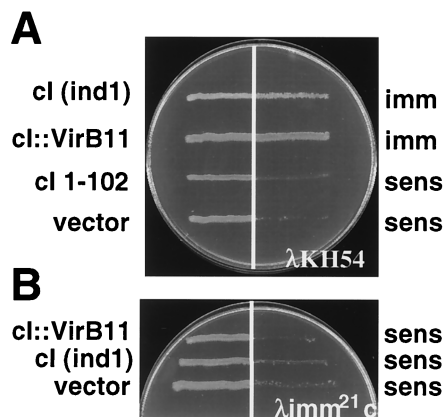


FIG. 3. Cross-streak analysis of AG1688 expressing the chimera cI':*virB11*. (A) Cross-streak analyses against  $\lambda$ KH54. (B) Cross-streak analyses against  $\lambda$ imm<sup>21c</sup>. Repressor constructs are indicated at the left, and immunity (imm) or sensitivity (sens) to phage is indicated at the right. Constructs and corresponding plasmids: cI (ind1), pJH157; cI':*virB11*, pSR66; cI 1-102 (pKH101); vector, pZ150.

TABLE 2. Summary of interactions between VirB11 mutants<sup>a</sup>

Bait protein <sup>b</sup>	Prey protein <sup>c</sup>	Interaction detected <sup>d</sup>	
		IP	cI
Wild type			
VirB11	VirB11	Yes	Yes
GFP	VirB11	No	
Class I mutants, recessive			
VirB11	K175Q	Yes	Yes
VirB11	Δ174-176	Yes	Yes
K175Q	K175Q	Yes	
Δ174-176	Δ174-176	Yes	
Class II mutants			
Dominant, nonfunctional			
VirB11	I88T; I103T	Yes	Yes
VirB11	H269R	Yes	Yes
VirB11	I103T; M301L	Yes	Yes
Dominant, functional			
VirB11	I265	Yes	Yes
VirB11	L75F	Yes	Yes
VirB11	Q135E	Yes	Yes
VirB11	V258G	Yes	Yes
VirB11	V116I	Yes	Yes

<sup>a</sup> Assessed by coprecipitation from *A. tumefaciens* PC1000 extracts using anti-GFP antisera and cI repressor fusion assays.

<sup>b</sup> Fused to GFP for precipitation studies.

<sup>c</sup> Prey proteins were (i) cosynthesized with bait protein to assay for coprecipitation from *A. tumefaciens* extracts and (ii) fused to the cI DNA binding domain cI repressor fusion assays in *E. coli*.

<sup>d</sup> Assessed by coprecipitation (IP) and by resistance to λKH54 superinfection (cI).

to immunoprecipitation with anti-GFP antisera. The alleles also were fused in frame downstream of the portion of cI encoding the N-terminal DNA binding domain, and resulting *E. coli* strains were assayed for immunity to λKH54 superinfection. All of the mutant proteins coprecipitated with VirB11.343::GFP from *A. tumefaciens* extracts and also mediated immunity to λ phage when produced as cI fusions in *E. coli* (Table 2) (25). These findings support our model that these mutant proteins most probably exert their dominant effects by forming nonproductive complexes with native VirB11.

**VirB11 association with truncated derivatives.** Previously, we showed that an allele encoding the C-terminal half of VirB11 exerts negative dominance, whereas one encoding the N-terminal half is recessive (26). To test whether these truncation derivatives differ in the ability to interact with native VirB11, we fused the coding sequences for residues 1 to 157 and 157 to 343 to *gfp* and coexpressed the resulting chimeric genes with wild-type *virB11* in PC1000 cells. The VirB11[1-157]::GFP protein was detected by immunoblotting as one prominent polypeptide of 42 kDa immunoreactive with anti-VirB11 (Fig. 4A, lane 3) and anti-GFP (data not shown) antisera. The VirB11[157-343]::GFP fusion migrated as two immunoreactive species of ~44 and 41 kDa (Fig. 4A, lane 4), most probably because of proteolytic degradation since the 41-kDa species also was detected in extracts from cells expressing full-length VirB11::GFP (lane 1). PC1000 cells coexpressing alleles for native VirB11 and each of the truncated fusion derivatives were used for immunoprecipitation analyses with anti-GFP antiserum. Full-length VirB11 was precipitated from lysates of cells that coexpressed either hybrid protein and was not precipitated from lysates lacking these hybrid proteins (Fig. 4 and Table 3). In addition, the C-terminal half of VirB11

was not precipitated by VirB11[1-157]::GFP, and conversely, the N-terminal half of VirB11 was not precipitated by VirB11[157-343]::GFP (Table 3).

Portions of VirB11 were fused to cI repressor protein. AG1688(pSR61) and AG1688(pSR62) cells, synthesizing the hybrid proteins cI::VirB11[1-157] and cI::VirB11[157-343], respectively, both grew in the presence of λ phage, suggesting that these VirB11 truncation derivatives also can mediate cI dimerization. By contrast, AG1688(pSR63) and AG1688(pSR64) cells, synthesizing the fusions cI::VirB11[157-302] and cI::VirB11[245-343], respectively, were unable to confer resistance to λKH54 (Fig. 5). The failure of smaller N- or C-terminal fragments to support self-interaction could be due to their intrinsic instabilities or because they lack required sequence information for dimerization. Together, results of the immunoprecipitation and cI studies indicate that VirB11 possesses two domains, one in each half of the protein, that self-interact.

As shown above, full-length VirB11 interacted with all mutant proteins with dominant and recessive behaviors (Table 2). We next tested whether differences in activities of the N- and C-terminal self-interaction domains could account for the dominant and recessive behaviors of these mutants. PC1000 cells expressing VirB11[1-157]::GFP or VirB11[157-343]::GFP derivatives and one of the mutant proteins were used for immunoprecipitation analyses. The GFP fusion proteins precipitated each of the mutants exerting dominant effects, suggesting that these mutant proteins retain functional self-interaction domains in their N- and C-terminal halves (Table 3). This result was predicted, at least for the class III dominant mutants that exhibit wild-type function when synthesized in the absence of native VirB11 (37). Interestingly, however, VirB11[1-157]::GFP precipitated the two Walker A mutants with recessive effects, but VirB11[157-343]::GFP failed to precipitate these mutant proteins (Table 3). Thus, in contrast to the dominant mutants, the Walker A mutants apparently possess a functional

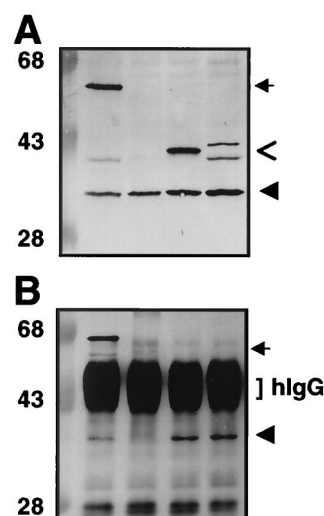


FIG. 4. Coprecipitation of VirB11 and VirB11 truncation derivatives fused to GFP. (A) TX-100-solubilized proteins subjected to SDS-PAGE and immunoblotted with anti-VirB11 antiserum. (B) Immunoprecipitates of protein extracts shown in panel A after immunoprecipitation with anti-GFP antiserum. Lanes: 1, PC1000(pSR70) expressing *virB11.343::gfp* and *virB11*; 2, PC1000(pED11) expressing *virB11*; 3, PC1000(pSR81) expressing *virB11[1-157]::gfp* and *virB11* (IncP plasmid); 4, PC1000(pSR82) expressing *virB11[157-343]::gfp* and *virB11*. hlgG, immunoreactive IgG heavy chain. Arrows indicate positions of VirB11.343::GFP, arrowheads identify VirB11, and open arrows identify VirB11 truncations fused to GFP. Positions of molecular weight markers are shown at the left, with sizes in kilodaltons indicated.

TABLE 3. Summary of interactions between VirB11 truncation derivatives<sup>a</sup>

Bait protein <sup>b</sup>	Prey protein <sup>c</sup>	Interaction detected?
VirB11	VirB11	Yes
[1-157]	VirB11	Yes
[157-343]	VirB11	Yes
[1-157]	[157-343]	No
[157-343]	[1-157]	No
Class I mutants, recessive		
[1-157]	K175Q	Yes
[1-157]	Δ174-176	Yes
[157-343]	K175Q	No
[157-343]	Δ174-176	No
Class II mutants		
Dominant, nonfunctional		
[1-157]	I88T; I103T	Yes
[157-343]	I88T; I103T	Yes
[1-157]	H269R	Yes
[157-343]	H269R	Yes
Dominant, functional		
[1-157]	I265	Yes
[157-343]	I265	Yes
[1-157]	L75F	Yes
[157-343]	L75F	Yes
[1-157]	Q1365E	Yes
[157-343]	Q135E	Yes
[1-157]	V258G	Yes
[157-343]	V258G	Yes

<sup>a</sup> Assessed by coprecipitation from *A. tumefaciens* PC1000 extracts using anti-GFP antisera.

<sup>b</sup> Fused to GFP for precipitation studies.

<sup>c</sup> Cosynthesized with bait protein to assay for coprecipitation from *A. tumefaciens* extracts.

N-terminal domain capable of mediating an interaction with VirB11[1-157]:GFP but a nonfunctional C-terminal domain that fails to interact with VirB11[157-343]:GFP. Because the Walker A and B motifs are located in the C terminus, these findings suggest that the C-terminal self-interaction domain is functional only in the context of ATP binding or hydrolysis.

## DISCUSSION

We are interested in defining how VirB11 is configured at the cytoplasmic membrane and the role it plays in macromolecular transport. Initial studies in this laboratory resulted in the isolation of a number of dominant VirB11 alleles. In all cases, dominance was at least partially suppressed by overproduction of any combination of VirB9, VirB10, and/or VirB11. A reasonable hypothesis to explain these suppression data is that the overproduction of proteins that interact directly or indirectly with VirB11 resulted in sequestration of the mutant proteins into nonproductive complexes (38). A study by the Binns laboratory supplied independent evidence for interactions between VirB9, VirB10, and VirB11 and further indicated that these proteins might act stoichiometrically and be rate-limiting for transporter assembly (36).

Our early studies of the dominant alleles showed that they fell into two classes. The class II mutations abolished protein functionality, as judged by a failure of the corresponding alleles to complement a ΔVirB11 mutation in virulence assays. By contrast, the class III mutations exerted strong negative dominance when alleles were coexpressed with VirB11 but encoded functional proteins when synthesized in the absence of the

native protein. The observation that these mutant proteins displayed a phenotype only when coexpressed with native VirB11 led to a model that VirB11 functions as a homomultimer (38). In the present study, we gained further evidence for VirB11 self-association in vivo. Precipitation studies revealed an interaction between native VirB11 and a VirB11::GFP fusion protein, and cI repressor fusion studies demonstrated the capacity of cI::VirB11 to dimerize. Interactions also were detected between full-length VirB11 and class II and III mutants exerting dominant effects as well as with Walker A mutants with recessive effects. For each of the observed interactions, complex formation clearly occurred independently of other VirB proteins, as demonstrated by the fact the complexes were recovered from *A. tumefaciens* mutants deleted of the remaining *virB* genes or they were detected in *E. coli*.

Both classes of dominant mutations were previously reported to be conservative substitutions that map to two fairly discrete regions of VirB11, one immediately upstream of the Walker A motif in the N-terminal half of the protein and the second in the C-terminal half of the protein (38). These findings led to the proposal that these regions might correspond to domains that mediate VirB11 complex formation. In support of this view, here we showed that both halves of VirB11 indeed are capable of interacting with the full-length protein. Furthermore, each half of VirB11 interacted with itself but not with the other half of the protein. Thus, as a working model we now propose that VirB11 self-assembles via N-N and C-C domain interactions.

Our present investigations have not revealed any differences between the class II and III dominant mutant proteins with respect to the capacity to self-assemble. Both classes of mutant proteins mediated dimerization of the DNA binding domain of cI repressor and coprecipitated with full-length VirB11 fused to GFP. Both classes also coprecipitated with the N- and C-terminal halves of VirB11 fused to GFP. Thus, we predict that in merodiploid cells the class II and III mutants dimerize with wild-type VirB11, but these mixed multimers arrest at some later stage in the transporter biogenesis pathway. Similarly, dimers of class II mutants that assemble in cells devoid of native VirB11 likely are dead-end complexes. However, the class III dimers that assemble in cells lacking native VirB11 must be competent for progression along the transporter biogenesis pathway. Given the clustering and the conservative nature of the class II and III substitutions (38), it is likely that

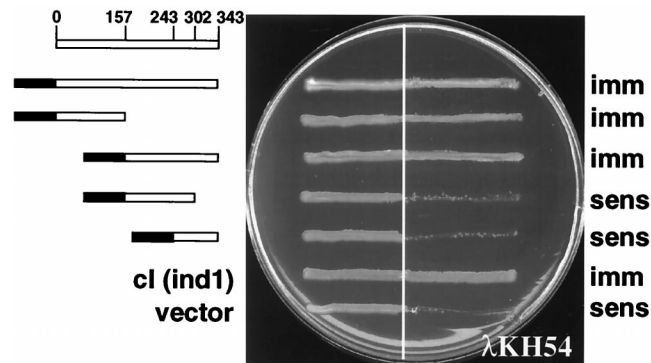


FIG. 5. Cross-streak analyses of AG1688 expressing cI repressor fusions to *virB11* deletion derivatives. Repressor constructs are indicated at the left, and immunity (imm) or sensitivity (sens) to phage is indicated at the right. Constructs and corresponding plasmids from top to bottom: cI::VirB11, pSR66; cI::VirB11 [1-157], pSR61; VirB11[157-343], pSR62; cI::VirB11[157-302], pSR63; cI::VirB11 [245-343], pSR64; cI::cIind1, pJH157; vector, pZ150.

the different behaviors of these mutants can be attributed to small perturbations of charge or conformation that render the class II homomultimers, but not the class III homomultimers, nonfunctional. Although our model proposes the dominant mutations affect transporter assembly, it is also possible these mutations impair the ability of a fully assembled transporter to dock or translocate substrate.

Our studies with the Walker A mutants revealed fundamentally different requirements for the N- and C-terminal regions of VirB11 to promote self-interaction. Whereas the N-terminal portion of VirB11 was able to multimerize with mutant proteins exhibiting dominant or recessive effects, the C-terminal portion failed to interact with the recessive Walker A mutants. These findings strongly suggest that ATP binding or hydrolysis is required for self-interaction via the C-terminal domain. We propose that nucleotide binding is required to induce a conformation appropriate for productive self-interaction. The ATP dependence of the C-terminal interaction domain offers a possible explanation for the recessive behaviors of VirB11 mutants. If, as predicted, ATP binding or hydrolysis is a critical reaction during transporter morphogenesis, mutants defective in this reaction might fail to interact with other VirB proteins and thus enter the morphogenetic pathway. In support of this view, an allele encoding the N-terminal half of VirB11, which lacks the nucleotide-binding motif, is recessive, whereas one encoding a C-terminal half with intact nucleotide binding motif is dominant (26). Of further possible significance, we have shown that Walker A mutants accumulate at appreciably lower levels than the wild-type protein even when overexpressed from an IncP replicon whose copy number exceeds that of the Ti plasmid 5- to 10-fold (25, 26). Presumably, complexes composed of Walker A mutant proteins are unstable and rapidly degraded. By analogy, several VirB proteins, including wild-type VirB11, have been shown to be unstable in various *virB* null mutants that show defects in transporter assembly (1, 15).

VirB11 and PulE are paradigmatic members of a superfamily of ATPases associated with macromolecular trafficking. Collectively, members of this superfamily contribute to motility, the secretion of virulence factors, and the assembly of sex and adhesive pili via secretion pathways that are now designated as types II and IV (2, 5, 8, 23, 24, 35). In fact, a comparison of the VirB11-related proteins with the ProDom protein domain program (<http://www.toulouse.inra.fr/prodom.html>) shows that a region corresponding to the N-terminal ~120 residues of the VirB11 is highly related to N-terminal regions of proteins associated with type IV transport but is considerably less related to the N-terminal regions of PulE and other ATPases associated with type II transport. By contrast, the C-terminal halves of all VirB11- and PulE-like proteins are highly homologous. It is interesting to speculate that the functional and, possibly, structural relatedness of these protein families is limited to their C-terminal nucleotide binding pockets.

Recent progress has been made toward definition of oligomeric structures of several traffic ATPases. There now is considerable evidence that the ATPase subunits of the ABC transporter superfamily assemble as dimers in which the monomers cooperatively interact to catalyze transport (9, 10, 30). Similarly, SecA translocase functions as a dimer (12). Multimerization also was demonstrated for two VirB11-like ATPases associated with type II secretion, PulE, an essential component of the *Klebsiella oxytoca* pullulanase secretion machinery (24), and *Pseudomonas aeruginosa* XcpR, also required for type II protein secretion (34). Interestingly, PulE migrates in non-reducing SDS-polyacrylamide gels as higher-order disulfide-cross-linked homo-oligomers (24). We similarly have observed that VirB11 forms disulfide-cross-linked complexes upon elec-

trophoresis of cell extracts under nonreducing conditions (25, 26). It is not known for either PulE or VirB11 whether these cross-links form *in vivo* or immediately upon cell lysis. Nevertheless, identification of these cross-linked complexes is consistent with the notion that both ATPases assemble as higher-order homomultimers *in vivo*.

Recently, Krause et al. (20, 20a) provided a possible architecture for the VirB11-like ATPases. Electron microscopy studies revealed that the TrbB ATPase from the IncP plasmid RP4, TrwD of plasmid R388, and HP0525 of *H. pylori* form homohexameric donut-shaped complexes (20, 20a). Further, gel filtration studies revealed differences in the oligomeric state of TrbB in the presence and absence of ATP. Thus, consistent with results from our studies of the VirB11 Walker A mutants, ATP binding appears to be critical for TrbB oligomerization. Current efforts in our laboratory are aimed at defining the stoichiometry of VirB11 oligomers and determining whether VirB11 also forms oligomeric rings. A complicating aspect of these studies is that in contrast to TrbB, which is cytosolic and quite soluble in solution, VirB11 is almost exclusively tightly membrane associated and readily aggregates in solution (6, 25, 26, 38).

#### ACKNOWLEDGMENTS

We thank members of the laboratory for helpful discussions, William Margolin for anti-GFP antiserum and GFP constructs, and Jim Hu for the  $\text{cI}$  repressor fusion system and helpful suggestions.

This work was supported by NIH grant GM48746.

#### REFERENCES

- Berger, B. R., and P. J. Christie. 1994. Genetic complementation analysis of the *Agrobacterium tumefaciens virB* operon: *virB2* through *virB11* are essential virulence genes. *J. Bacteriol.* **176**:3646–3660.
- Burns, D. L. 1999. Biochemistry of type IV secretion. *Curr. Opin. Microbiol.* **2**:25–29.
- Chen, C.-Y., and S. C. Winans. 1991. Controlled expression of the transcriptional activator gene *virG* in *Agrobacterium tumefaciens* by using the *Escherichia coli lac* promoter. *J. Bacteriol.* **173**:1139–1144.
- Christie, P. J. 1997. The *Agrobacterium tumefaciens* T-complex transport apparatus: a paradigm for a new family of multifunctional transporters in eubacteria. *J. Bacteriol.* **179**:3085–3094.
- Christie, P. J., and J. P. Vogel. Bacterial type IV secretion: conjugation systems adapted for delivery of effector molecules to host cells. *Trends Microbiol.*, in press.
- Christie, P. J., J. E. Ward, S. C. Winans, and E. W. Nester. 1989. A gene required for transfer of T-DNA to plants encodes an ATPase with autophosphorylating activity. *Proc. Natl. Acad. Sci. USA* **86**:9677–9681.
- Dang, T. A., X.-R. Zhou, B. Graf, and P. J. Christie. 1999. Dimerization of the *Agrobacterium tumefaciens* VirB4 ATPase and the effect of ATP-binding cassette mutations on assembly and function of the T-DNA transporter. *Mol. Microbiol.* **32**:1239–1253.
- Das, A. 1998. DNA transfer from *Agrobacterium* to plant cells in crown gall tumor disease. *Subcell. Biochem.* **29**:343–363.
- Davidson, A., S. Laghaecian, and D. Mannering. 1996. The maltose transport system of *Escherichia coli* displays positive cooperativity in ATP hydrolysis. *J. Biol. Chem.* **271**:4858–4863.
- Davidson, A. L., and S. Sharma. 1997. Mutation of a single MalK subunit severely impairs maltose transport activity in *Escherichia coli*. *J. Bacteriol.* **179**:5458–5464.
- de Groot, M. J. A., P. Bundock, P. J. J. Hooikaas, and A. G. M. Beijersbergen. 1998. *Agrobacterium tumefaciens*-mediated transformation of filamentous fungi. *Nat. Biotechnol.* **16**:839–842.
- Driessen, A. J. 1993. SecA, the peripheral subunit of the *Escherichia coli* precursor protein translocase, is functional as a dimer. *Biochemistry* **32**:13190–13197.
- Eisenbrandt, R., M. Kalkum, E. M. Lai, R. Lurz, C. I. Kado, and E. Lanka. 1999. Conjugative pili of IncP plasmids, and the Ti plasmid T pilus are composed of cyclic subunits. *J. Biol. Chem.* **274**:22548–22555.
- Fernandez, D., T. A. T. Dang, G. M. Spudich, X.-R. Zhou, B. R. Berger, and P. J. Christie. 1996. The *Agrobacterium tumefaciens virB7* gene product, a proposed component of the T-complex transport apparatus, is a membrane-associated lipoprotein exposed at the periplasmic surface. *J. Bacteriol.* **178**:3156–3167.
- Fernandez, D., G. M. Spudich, X.-R. Zhou, and P. J. Christie. 1996. The *Agrobacterium tumefaciens* VirB7 lipoprotein is required for stabilization of



- VirB proteins during assembly of the T-complex transport apparatus. *J. Bacteriol.* **178**:3168–3176.
16. **Garfinkel, D. J., R. B. Simpson, L. W. Ream, F. F. White, M. P. Gordon, and E. W. Nester.** 1981. Genetic analysis of crown gall: fine structure map of the T-DNA by site-directed mutagenesis. *Cell* **27**:143–153.
  17. **Hu, J.** 1995. Repressor fusions as a tool to study protein-protein interactions. *Structure* **3**:431–433.
  18. **Hu, J., M. Kornacker, and A. Hochschild.** 2000. *Escherichia coli* one- and two-hybrid systems for the analysis and identification of protein-protein interactions. *Methods* **20**:80–94.
  19. **Klee, H. J., M. F. Yanofsky, and E. W. Nester.** 1985. Vectors for transformation of higher plants. *Bio/Technology* **3**:637–642.
  20. **Krause, S., M. Barcena, W. Pansegrau, R. Lurz, J. Carazo, and E. Lanka.** 2000. Sequence related protein export NTPases encoded by the conjugative transfer region of RP4 and by the *cag* pathogenicity island of *Helicobacter pylori* share similar hexameric ring structures. *Proc. Natl. Acad. Sci. USA* **182**:2761–2770.
  - 20a. **Krause, S., W. Pansegrau, R. Lurz, F. de la Cruz, and E. Lanka.** 2000. Enzymology of type IV macromolecule secretion systems: the conjugative transfer regions of plasmids RP4 and R388 and the *cag* pathogenicity island of *Helicobacter pylori* encode structurally and functionally related nucleoside triphosphate hydrolases. *J. Bacteriol.* **182**:2761–2770.
  21. **Lai, E. M., and C. I. Kado.** 1998. Processed VirB2 is the major subunit of the promiscuous pilus of *Agrobacterium tumefaciens*. *J. Bacteriol.* **180**:2711–2717.
  22. **Ma, X., D. W. Ehrhardt, and W. Margolin.** 1996. Colocalization of cell division proteins FtsZ and FtsA to cytoskeletal structures in living *Escherichia coli* cells by using green fluorescent protein. *Proc. Natl. Acad. Sci. USA* **93**:12998–13003.
  23. **O'Callaghan, D., C. Cazeville, A. Allardet-Servent, M. L. Boschioli, G. Bourg, V. Foulongne, P. Frutos, Y. Kulakov, and M. Ramuz.** 1999. A homologue of the *Agrobacterium tumefaciens* VirB and *Bordetella pertussis* Ptl type IV secretion systems is essential for intracellular survival of *Brucella suis*. *Mol. Microbiol.* **33**:1210–1220.
  24. **Possot, O., and A. Pugsley.** 1994. Molecular characterization of PulE, a protein required for pullulanase secretion. *Mol. Microbiol.* **12**:287–299.
  25. **Rashkova, S.** 1998. Studies of subcellular localization and complex formation of the *Agrobacterium tumefaciens* transport ATPase VirB11. Ph.D. thesis. The University of Texas—Houston Medical School, Houston.
  26. **Rashkova, S., G. M. Spudich, and P. J. Christie.** 1997. Mutational analysis of the *Agrobacterium tumefaciens* VirB11 ATPase: identification of functional domains and evidence for multimerization. *J. Bacteriol.* **179**:583–589.
  27. **Rivas, S., S. Bolland, E. Cabezon, F. M. Goni, and F. de la Cruz.** 1997. TrwD, a protein encoded by the IncW plasmid R388, displays an ATP hydrolase activity essential for bacterial conjugation. *J. Biol. Chem.* **272**:25583–25590.
  28. **Salmund, G. P. C.** 1994. Secretion of extracellular virulence factors by plant pathogenic bacteria. *Annu. Rev. Phytopathol.* **32**:181–200.
  29. **Schmidt-Eisenlohr, H., N. Domke, C. Angerer, G. Wanner, P. C. Zambryski, and C. Baron.** 1999. Vir proteins stabilize VirB5 and mediate its association with the T pilus of *Agrobacterium tumefaciens*. *J. Bacteriol.* **181**:7485–7492.
  30. **Schneider, E., and S. Hunke.** 1998. ATP-binding-cassette (ABC) transport systems: functional and structural aspects of the ATP-hydrolyzing subunits/domains. *FEMS Microbiol. Rev.* **22**:1–20.
  31. **Segal, E., J. Cha, J. Lo, S. Falkow, and L. Tompkins.** 1999. Altered states: involvement of phosphorylated CagA in the induction of host cellular growth changes by *Helicobacter pylori*. *Proc. Natl. Acad. Sci. USA* **96**:14559–14564.
  32. **Segal, G., and H. A. Shuman.** 1998. How is the intracellular fate of the *Legionella pneumophila* phagosome determined? *Trends Microbiol.* **6**:253–255.
  33. **Stein, M., R. Rappuoli, and A. Covacci.** 2000. Tyrosine phosphorylation of the *Helicobacter pylori* CagA antigen after *cag*-driven host cell translocation. *Proc. Natl. Acad. Sci. USA* **97**:1263–1268.
  34. **Turner, L. R., J. W. Olson, and S. Lory.** 1997. The XcpR protein of *Pseudomonas aeruginosa* dimerizes via its N-terminus. *Mol. Microbiol.* **26**:877–887.
  35. **Vogel, J. P., and R. R. Isberg.** 1999. Cell biology of *Legionella pneumophila*. *Curr. Opin. Microbiol.* **2**:30–34.
  36. **Ward, J. E. J., E. M. Dale, P. J. Christie, E. W. Nester, and A. N. Binns.** 1990. Complementation analysis of *Agrobacterium tumefaciens* Ti plasmid *virB* genes by use of a *vir* promoter expression vector: *virB9*, *virB10*, and *virB11* are essential virulence genes. *J. Bacteriol.* **172**:5187–5199.
  37. **Watson, B., T. C. Currier, M. P. Gordon, M. D. Chilton, and E. W. Nester.** 1975. Plasmid required for virulence of *Agrobacterium tumefaciens*. *J. Bacteriol.* **123**:255–264.
  38. **Zhou, X.-R., and P. J. Christie.** 1997. Suppression of mutant phenotypes of the *Agrobacterium tumefaciens* VirB11 ATPase by overproduction of VirB proteins. *J. Bacteriol.* **179**:5835–5842.
  39. **Zhou, X.-R., and P. J. Christie.** 1999. Mutagenesis of *Agrobacterium* VirE2 single-stranded DNA-binding protein identifies regions required for self-association and interaction with VirE1 and a permissive site for hybrid protein construction. *J. Bacteriol.* **181**:4342–4352.
  40. **Zupan, J., D. Ward, and P. Zambryski.** 1998. Assembly of the VirB transport complex for DNA transfer from *Agrobacterium tumefaciens* to plant cells. *Curr. Opin. Microbiol.* **1**:649–655.